Journal of Sound and Vibration (2001) **244**(4), 615–634
doi:10.1006/jsvi.2000.3497, available online at http://www.idealibrary.com on IDEAL®

PERFORMANCE EVALUATION OF MULTICHANNEL ADAPTIVE ALGORITHMS FOR LOCAL ACTIVE NOISE CONTROL

M. DE DIEGO AND A. GONZALEZ

Department of Communicaciones, Universidad Politecnica de Valencia, Camino de Vera s/n, E-46022, Valencia, Spain. E-mail: mdediego@dcom.upv.es

(*Received* 4 *November* 1999, *and in final form* 8 *August* 2000)

This paper deals with the development of a multichannel active noise control (ANC) system inside an enclosed space. The purpose is to design a real practical system which works well in local ANC applications. Moreover, the algorithm implemented in the adaptive controller should be robust, of low computational complexity and it should manage to generate a uniform useful-size zone of quite in order to allow the head motion of a person seated on a seat inside a car. Experiments were carried out under semi-anechoic and listening room conditions to verify the successful implementation of the multichannel system. The developed prototype consists of an array of up to four microphones used as error sensors mounted on the headrest of a seat place inside the enclosure. One loudspeaker was used as single primary source and two secondary sources were placed facing the seat. The aim of this multichannel system is to reduce the sound pressure levels in an area around the error sensors, following a local control strategy. When using this technique, the cancellation points are not only the error sensor positions but an area around them, which is measured by using a monitoring microphone. Different multichannel adaptive algorithms for ANC have been analyzed and their performance verified. Multiple error algorithms are used in order to cancel out different types of primary noise (engine noise and random noise) with several configurations (up to four channels system). As an alternative to the *multiple error LMS* algorithm (multichannel version of the *filtered-X LMS* algorithm, MELMS), the *least maximum mean squares* (LMMS) and the *scanning error-LMS* algorithm have been developed in this work in order to reduce computational complexity and achieve a more uniform residual field. The ANC algorithms were programmed on a digital signal processing board equipped with a TMS320C40 floating point DSP processor. Measurements concerning real-time experiments on local noise reduction in two environments and at frequencies below 230 Hz are presented. Better noise levels attenuation is obtained in the semianechoic chamber due to the simplicity of the acoustic field. The size of the zone of quiet makes the system useful at relatively low frequencies and it is large enough to cover a listener's head movements. The spatial extent of the zones of quiet is generally observed to increase as the error sensors are moved away from the secondary source, they are put closer together or its number increases. In summary, different algorithms' performance and the viability of the multichannel system for local active noise control in real listening conditions are evaluated and some guidelines for designing such systems are then proposed.

1. INTRODUCTION

Active noise control (ANC) is a field of growing interest that combines digital signal processing techniques with traditional acoustics. ANC systems attempt to reduce the noise by generating an antinoise that cancels out the first one [1, 2]. In a structure like a duct, with only one relevant dimension, it is relatively easy to cancel travelling waves by placing

0022-460X/01/290615 + 20 $35.00/0

a secondary source of sound in a point of the duct and producing a destructive interference. A good level of attenuation can be achieved from the interference point onwards. Nevertheless, it is harder to cancel noise inside an enclosure because of the appearance of stationary waves. Those tri-dimensional stationary waves are known as the acoustic modes of the enclosure. The higher the working frequency the larger the number of acoustic modes excited [3]. There are points inside the enclosure where some modes cannot be excited and therefore these modes cannot be detected at these points. These null points are placed at different positions for each mode. Since practical active control systems interact with the system under control at certain points belonging to the real space, it is very difficult to achieve good results in an enclosure by using a single channel ANC system. The use of several sources and sensors avoids these problems by introducing some degree of spatial diversity. A way to control actively a noise in an enclosure consists in trying to minimize the whole acoustic potential energy [2]. This potential energy is proportional to the volume integral of the sound pressure mean square value. Sound pressure at low frequencies can be represented by a combination of a given number of acoustic modes. A good estimate of the acoustic potential energy in the enclosure could be the sum of the mean square pressures measured at many different points in the room. The quality of this approach depends on the location and number of sensors that have been used, since it should be possible to measure the contributions of all the relevant modes at the working frequencies by increasing this number. For example, in a rectangular enclosure it would be advisable to place the sensors, and also the cancelling sources, near the corners, since all the modes have a maximum there.

When the number of sensors is large enough, the multichannel system is able to reduce the acoustic potential energy in the enclosure. The strategy is known as global control. If the number of sensors is smaller then it will be possible to reduce the sound pressure in an area around the sensors; however, the noise levels could even increase outside this area [2, 4]. This strategy, which is called local control, is a low-cost solution that is acceptable in some ANC applications [5]. For example, when considering the interior space of an automobile, noise reduction is required only in the space where the heads of driver and passengers are normally located. Quiet zones have been evaluated in the literature and they have typically a diameter larger than a quarter of the working wavelength. At low frequencies, these zones of quiet are large enough for covering lateral and forward listener's head movements [6]. However, it is important to optimize the number and location of the secondary loudspeakers and error sensor microphones in order to maximize the size of the quiet zones. It is also convenient to analyze the residual field distribution in the cancellation zone, since it can be shown that uniformity of the residual field improves the comfort sensation. Therefore, a local control strategy has been applied to the ANC system presented here and two characteristics of the acoustic field have been mainly evaluated: extension of the quiet zone after control and uniformity of the residual field.

In order to look for an algorithm which was robust, of low computational complexity and that provides useful-size zones of quiet, three different adaptive signal processing algorithms for active noise control have been considered in this paper. These algorithms are: multichannel *filtered-X* LMS (commonly named MELMS) [7], *least maximum mean squares* (LMMS) [8] and *scanning error-LMS* [9] algorithms. They are steepest descent-type algorithms and, as it happens with LMS, they have shown to be robust and have good tracking capabilities. The multichannel filtered-X LMS algorithm can be considered the most representative of this kind because it is widely used. It minimizes the sum of the squares of the measured signals. This strategy produces a residual acoustic field in the enclosure that can have large differences between the values of its maximum and minimum levels. In most applications, a more uniform acoustic field is desired, since

a difference of levels could be easily perceived by a person walking inside a room. As an alternative to this algorithm, least maximum mean squares and scanning error-LMS algorithms have been developed and applied in this work in order to reduce computational complexity. Moreover, LMMS can achieve in some cases a more uniform residual field [10, 11]. All the algorithms have been tested in the same real conditions.

The complexity of LMMS and scanning error-LMS algorithms is significantly smaller than those of other adaptive filtering algorithms such as the recursive least squares (RLS) type algorithms or the least squares lattice (LSL) algorithm, which can increase convergence rate with random noise signals. A block processing technique has been recently proposed to reduce computational complexity of the MELMS algorithm, see reference [12], being under development in multichannel configuration. Recent literature has shown some examples of active noise control systems: in reference [13] a multichannel LSL algorithm is proposed to control road noise inside a car and in reference [14] a multichannel system with feedback–feedforward configuration based on the filtered-X LMS algorithm can be found. Unfortunately, both papers present only simulations, but not practical results. In reference [15] an approach to simulate the performance of ANC systems using filtered-X type algorithms is developed. An interesting work related to experiments in *personal* sound (different sound zones are required for different listeners in the same room), including local active noise control with a multichannel filtered-X LMS algorithm, is presented in reference [16].

The application of the filtered-X LMS, LMMS and scanning error-LMS algorithms in a multichannel system is in-depth investigated in this work by means of analytical results and laboratory experiments. The practical system implemented in the laboratory is also described. This system is designed to control noise around the headrest of a seat. Some of the practical aspects of its implementation are also considered: appropriate positioning of the secondary loudspeakers and error microphones, performance in different acoustic environments (different rooms and different noise disturbances) and sampling rate. The paper shows some results concerning real-time experiments on local noise reduction with random noise and engine noise as primary signal when using different configurations of loudspeakers and microphones and the aforementioned algorithms. The quiet zones are presented. Results show that quiet zones are large enough to allow slight head movements of the seated person without significant performance degradation.

The paper proceeds as follows: section 2 describes the multichannel adaptive algorithms used in the controller; the local active noise control prototype is described in section 3 and finally, the experimental results are reported in section 4.

2. MULTICHANNEL ADAPTIVE ALGORITHMS FOR ACTIVE NOISE CONTROL

Steepest descent algorithms are often applied to real-time systems and they have been widely used for active control. These iterative algorithms update the parameters of the controller following the direction of the negative gradient vector (that is in the direction of steepest descent with respect to these parameters of the error-performance surface) [10, 17]. The following algorithms have been developed based on the steepest-descent method and the stochastic gradient approach as shown in reference [10].

Multichannel filtered-X LMS algorithm. Least mean squares (LMS) algorithm minimizes the instantaneous signal error power; its active noise control version is called the *filtered-X LMS* algorithm [18]. The multichannel *filtered-X LMS* algorithm is commonly called the *multiple error LMS* (MELMS) [7].

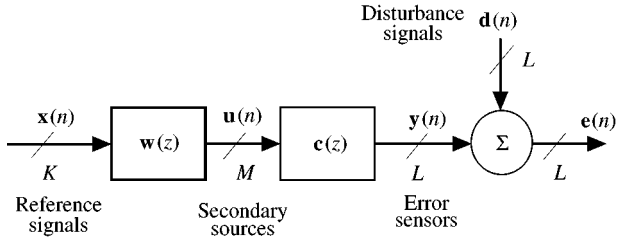

Figure 1. Multichannel pure feedforward ANC system. The system has M secondary sources, K reference signals and L error sensors (De-Diego and Gonzalez).

Scanning error-LMS algorithm. This algorithm, which was proposed in reference [9], appears as a computationally efficient version of the LMS algorithm. It updates the control filter weights using only a number of error signals at each algorithm iteration. It has been studied in reference [19].

Least maximum mean squares algorithm. This algorithm, denoted as LMMS, strives to reduce the error signal with maximum level. It belongs to a kind of algorithm called minimax type which was studied in references [8, 10, 11]. The aim behind a minimax-type algorithm in active control is to balance the acoustic field after control. To achieve this, it is needed to define first which measure of the acoustic field must be balanced and then apply a minimax strategy of minimization using this measure. When the maximum of the mean squared values of the error signals is minimized, the algorithm is called least maximum mean squares (LMMS).

2.1. MULTICHANNEL FILTERED-X LMS ALGORITHM (MELMS)

The multichannel version of the filtered-X LMS algorithm is called the multiple error LMS algorithm (MELMS) [6, 7]. A system with K reference signals, M secondary sources and L error sensors as in reference [20] will be considered. Figure 1 shows the block diagram of this model. Block C represents a matrix of $L \times M$ error paths (transfer functions from each secondary source to each error sensor) and block W is a matrix of $K \times M$ control filters that are designed to minimize the sum of the squares of L error sensor outputs (the system under control is considered time invariant). Primary noise is actively cancelled out by using the M secondary signals which are fed by the $K \times M$ adaptive filters. The output of the lth error sensor can then be written as

$$e_l[n] = d_l[n] + \sum_{k=1}^{K} \sum_{m=1}^{M} \sum_{j=0}^{J-1} c_{lmj} \sum_{i=0}^{I-1} w_{mki} x_k[n-i-j], \tag{1}$$

where $d_l[n]$ is the primary noise at the lth error sensor, c_{lmj} is the jth coefficient of the impulse response from the mth secondary source to the lth error sensor. The last summation represents the kth reference signal filtered through the corresponding adaptive finite impulse response filter of I coefficients. Equation (1) illustrates the linear relationship between the error signal and the controller coefficients and can also be expressed in matrix form as

$$\mathbf{e}[n] = \mathbf{d}[n] + \mathbf{R}[n]\mathbf{w}, \tag{2}$$

where $\mathbf{R}[n]$ is the filtered reference signals matrix. Parameters involved in equation (1) are defined as

$$\mathbf{e}[n] = [e_1[n], e_2[n], \ldots, e_L[n]]^{\mathrm{T}}, \tag{3}$$

$$\mathbf{d}[n] = [d_1[n], d_2[n], \ldots, d_L[n]]^{\mathrm{T}}, \tag{4}$$

$$\mathbf{w} = [\mathbf{w}_0^{\mathrm{T}}, \mathbf{w}_1^{\mathrm{T}}, \ldots, \mathbf{w}_{I-1}^{\mathrm{T}}]^{\mathrm{T}} \tag{5}$$

with

$$\mathbf{w}_i = [w_{11i}, w_{12i}, \ldots, w_{MKi}]^{\mathrm{T}} \tag{6}$$

and

$$\mathbf{R}[n] = \begin{bmatrix} \mathbf{r}_1^{\mathrm{T}}[n] & \mathbf{r}_1^{\mathrm{T}}[n-1] & \cdots \\ \mathbf{r}_2^{\mathrm{T}}[n] & \mathbf{r}_2^{\mathrm{T}}[n-1] & \cdots \\ \cdot & \cdot & \cdots \\ \cdot & \cdot & \cdots \\ \cdot & \cdot & \mathbf{r}_L^{\mathrm{T}}[n-I+1] \end{bmatrix}$$

with

$$\mathbf{r}_l[n] = [r_{l11}[n], \tau_{l12}[n], \ldots, \tau_{lMK}[n]]^{\mathrm{T}}. \tag{7}$$

The optimum value of the coefficient vector $\mathbf{w}$ minimizes the cost function

$$J = E\left[\sum_{l=1}^{L} \{e_l[n]\}^2\right], \tag{8}$$

where $E[\cdot]$ denotes an expected value. If the reference signal $x_k[n]$ is correlated with $d[n]$, it is possible to reduce the value of J by driving the secondary sources by a filtered version of the reference signal. Since the gradient vector of the cost function is difficult to calculate in practice, the optimum set of filters coefficients required to minimize equation (8) may be evaluated iteratively by using the steepest descent algorithm which uses a stochastic estimation of the cost function gradient vector,

$$\mathbf{w}[n+1] = \mathbf{w}[n] - \alpha \sum_{l=1}^{L} \mathbf{R}_l^{\mathrm{T}}[n] e_l[n], \tag{9}$$

where α is the convergence parameter and $\mathbf{R}_l[n]$ corresponds to the lth row of the filtered reference signals matrix $\mathbf{R}[n]$.

Two of the best-known applications of the multiple error LMS algorithm are the control of *boom* noise in cars [21] and the control of propeller-induced noise in flight cabin interiors [22]. An interesting convergence analysis of the MELMS algorithm has been reported in reference [23]. Alternative methods for reducing the computational complexity and memory requirements of the multichannel adaptive controller have also been developed [24, 25].

2.2. LEAST MAXIMUM MEAN SQUARES (LMMS) ALGORITHM

A more general cost function than the previous one, equation (8), can be derived from the error signals. This cost function is the p-norm of a vector composed of these signals, (see reference [10]):

$$J_p = E\left[\sum_{l=1}^{L} |e_l[n]|^p\right]. \tag{10}$$

Different values of the parameter p lead one from the minimization of the sum of the squares, $p = 2$ (which gives the MELMS algorithm), to the minimization of the maximum measured signal at each n, in the limiting case with p tending to ∞. A more uniform residual field can be obtained for larger values of p. The study here is focussed on the limiting case, in which only one of the error signals is used in the algorithm's calculations at each n. Therefore, the computational load can also be reduced. A closed expression for the coefficients vector which minimizes equation (10) does not seem to exist for the general case, but does exist for $p = 2$ which provides the MELMS cost function. In any case, an iterative expression to minimize J_p based on a steepest descent method can be used to reach this optimum. The true gradient vector of the cost function is approximated by a stochastic estimation. The stochastic gradient vector is then given by

$$\frac{\partial J_p[n]}{\partial \mathbf{w}} = \sum_{l=1}^{L} |e_l[n]|^{p-2}\, \mathbf{R}_l^{\mathrm{T}}[n] e_l[n]. \tag{11}$$

An iterative algorithm to minimize equation (10) is built by using the stochastic gradient definition in equation (11),

$$\mathbf{w}[n+1] = \mathbf{w}[n] - \alpha \sum_{l=1}^{L} |e_l[n]|^{p-1} \mathbf{R}_l^{\mathrm{T}}[n] \operatorname{sign}(e_l[n]), \tag{12}$$

where sign(.) is the sign function. When $p = 2$ equation (12) becomes

$$\mathbf{w}[n+1] = \mathbf{w}[n] - \alpha \sum_{l=1}^{L} \mathbf{R}_l^{\mathrm{T}}[n] e_l[n], \tag{13}$$

which is, as was expected, the same iterative expression as the definition of the multiple error LMS algorithm; see equation (9).

The limiting case, $p \to \infty$, has in general no sense with equation (11). The point is that the sum of the ∞ order moments of the error signals is not what really must be minimized. The minimax type algorithms in active control try to balance the acoustic field after control by applying a minimax strategy of minimization. A cost function definition that takes into account the last discussion is

$$J_\infty(q) = \lim_{p\to\infty} \sqrt[p]{\sum_{1 \leqslant l \leqslant L} \{E[|e_l[n]|^q]\}^p} = \max_{1 \leqslant l \leqslant L} E[|e_l[n]|^q] = E[|e_b[n]|^q], \tag{14}$$

where $q > 0$ is a parameter which can be selected to change the error signals measure. This measure is given in equation (14) by the error signals q order moments. Subscript b selects between the error signals, $1 \leqslant l \leqslant L$, the one with larger q order moment. It is interesting to note that the value of subscript b depends on the current value of the coefficients vector $\mathbf{w}$; a change of this vector could imply a change of the value of b. The instantaneous value of

equation (14),

$$J_\infty[n, q] = \max_{1 \leqslant l \leqslant L} \{|e_l[n]|^q\} = |e_b[n]|^q, \tag{15}$$

is used to obtain the stochastic gradient of the cost function,

$$\frac{\partial J_\infty[n, q]}{\partial \mathbf{w}} = q|e_b[n]|^{q-2}\mathbf{R}_b^{\mathrm{T}}[n]e_b[n]. \tag{16}$$

It has really practical sense for the case with $q = 2$ since the second order moments of the error signals are easily related to physical quantities whose mean squared value has practical sense. That is the main idea of the least maximum mean squares algorithm, LMMS. The LMMS algorithm [11] is an iterative steepest-descent algorithm that minimizes the maximum of the mean squared value of the error signals. This fact implies that the algorithm works with as many error-performance surfaces as error sensors. To find the minimum value of the maximum mean squared error the algorithm is descending for only one error-performance surface, a different one depending on which error sensor gives the maximum power at each algorithm iteration. The stochastic cost function consists of the instantaneous maximum value of the error signals as follows (see equation (15) with $q = 2$):

$$J[n] = \max_{1 \leqslant l \leqslant L} \{(e_l[n])^2\} = (e_b[n])^2. \tag{17}$$

Therefore, upon using the stochastic gradient the update weights equation is given by

$$\mathbf{w}[n + 1] = \mathbf{w}[n] - \alpha\mathbf{R}_b^{\mathrm{T}}[n]e_b[n], \tag{18}$$

where subscript b denotes the error signal with maximum squared value for a given value of the control vector. Equation (18) is quite similar to equation (9); however, summation over all the error sensors in equation (9) has disappeared in equation (18), and consequently a significant computational saving from this point of view has been obtained. However, a comparison between the error signal magnitudes has to be additionally carried out. This fact means that the LMMS algorithm has to find out which of the error signals have the maximum estimated mean power, although there exist efficient methods for this calculation. In this work, the mean power of the error signals was calculated by means of an IIR filtering of the error powers [11] as follows,

$$\hat{P}_e[n + 1] = \alpha\hat{P}_e[n] + (1 - \alpha)e^2[n], \tag{19}$$

where the parameter α is called the forgetting factor and it is typically chosen as $0{\cdot}91 \leqslant \alpha \leqslant 0{\cdot}94$. It is important to note that, even though the algorithm update equations are similar, MELMS and LMMS do not minimize the same cost function. Therefore, a different residual acoustic field after cancellation can be expected.

2.3. SCANNING ERROR-LMS ALGORITHM

The scanning error-LMS algorithm is an efficient version of the MELMS algorithm that also allows computational savings. It has been shown that this algorithm converges to the same solution as the MELMS under certain conditions [9, 19]. However, this algorithm, similar to the LMMS, can work using only one error signal at each algorithm iteration. This

TABLE 1

Computational complexity (Operations per Sample) in a $1 \times M \times L$ multichannel ANC system using the MELMS, LMMS and scanning error-LMS algorithms

	MELMS	LMMS	Scanning
Multiplications	$((JI + 1)L + 1)M$	$(JI + 2)M + 3L$	$(JI + 2)M$
Additions	$((J - 1)IL + 1)M$	$((J - 1)I + 1)M + 2L$	$((J - 1)I + 1)M$

error signal is chosen in turn (unlike LMMS which minimizes the maximum instantaneous power signal). The instantaneous cost function is defined as

$$J[n] = (e_b[n])^2, \tag{20}$$

where the error signal index b is defined as $b = n + 1 \bmod L$, so the error signals are scanned in turn. When the number of error sensors is large, the number of operations in the MELMS algorithm grows considerably. On the other hand, there does not exist this dependence of computational load on the number of sensors when the scanning error-LMS is used. It can be shown that by using equation (20) the update equation of the adaptive filters for the scanning error-LMS algorithm is given by

$$\mathbf{w}[n + 1] = \mathbf{w}[n] - \mu \mathbf{R}_b^{\mathrm{T}}[n] e_b[n]. \tag{21}$$

Due to the update equation similarities, resemblance between LMMS and scanning error-LMS algorithm can be expected during their convergence times. More details can be found in references [10, 26]. The computational complexity of the miltichannel ANC systems using the algorithms mentioned above is compared in Table 1. It is shown that multichannel configurations using the scanning error-LMS algorithm require much fewer operations per sampling period than those using the MELMS. The LMMS algorithm computational load depends on the number of error sensors. Its efficiency decreases as the number of error sensors increases due to the calculation of the error signal powers. For few error sensors, the computational load of the LMMS is comparable to that of the scanning error-LMS.

3. PROTOTYPE DESCRIPTION

A local active noise control system was used in the experiments. This ANC system was tested in two different acoustic environments: a rectangular enclosure with internal dimensions 4·35 m × 3·28 m × 2·96 m and a semi-anechoic chamber. The impulse responses and the transfer functions between two points of the two environments can be seen in Figure 2. Off-line modelling of the error signal paths are used in the experiments. Multichannel off-line modelling of error paths is a difficult task because of the acoustical coupling between the individual channels. Therefore, only one error path from one of the loudspeakers to one of the microphones can be estimated at a time. However, the error paths are time-varying due to the temperature variations and movement of objects. Consequently, on-line modelling of this error path could be considered for automotive application. The acoustic field will be more uniform in the semi-anechoic chamber than in the listening (real) room, due to its flatter frequency response compared to the real room

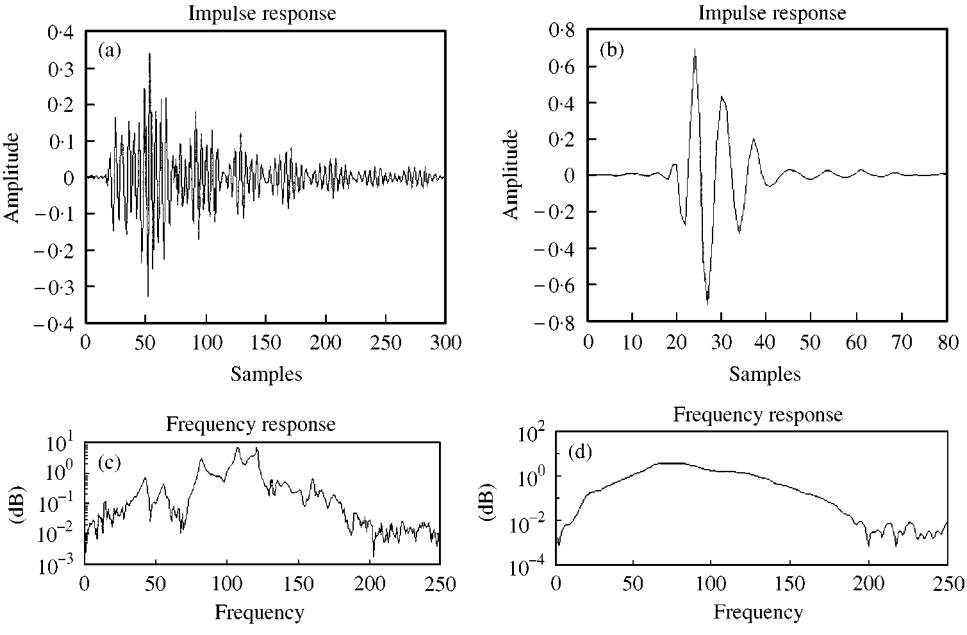

Figure 2. Examples of impulse and frequency responses between two points inside the environments used in the experiments: (a) and (c) real room and (b) and (d) semi-anechoic chamber. Sampling rate 500 Hz (De-Diego and Gonzalez).

one, which is quite abrupt. This character will make cancellation easier in the semi-anechoic environment.

For the results presented here, three 210 mm-diameter loudspeakers were used, a single one acted as primary source and the other loudspeakers were used as control sources. In the rectangular listening room, primary source was located at position (0·85, 1·5, 1) m and secondary source were located at positions (2·4, 2·3, 1·3) m and (2·4, 0·75, 1·3) m. A seat was placed at position (3·25, 1·6, 1·2) m, facing the primary source, and an array of up to four microphones was counted on the headrest of a seat, as shown in Figure 3. Pairs of error sensors are maintained at a distance between them given by S_x, S_y and S_z in the x, y and z co-ordinates respectively. The microphones and loudspeakers arrangement shown in Figure 3 is mainly used in the experiments. However, some other arrangements have also been used to test the performance of other configurations.

The working frequency range was 40–150 Hz in the rectangular enclosure and 40–230 Hz in the semi-anechoic chamber, since wider control bandwidth increased the number of adaptive control filters weights beyond our processing capabilities. Car engine noise (periodic noise) and random noise (broadband noise) were chosen as disturbances.

The ANC control algorithm was programmed on a digital signal processing (DSP) board equipped with a floating point DSP processor. The DSP board was mounted on a PC computer, which serves as a development system of the DSP board. The sampling rate was fixed at 500 Hz. All convergence rates in the experiments were adjusted to their optimal values so that the fastest convergence speed was achieved. Measurements obtained in both cases and for different transducers configurations show meaningful reductions in noise level at the sensor positions and the area around them.

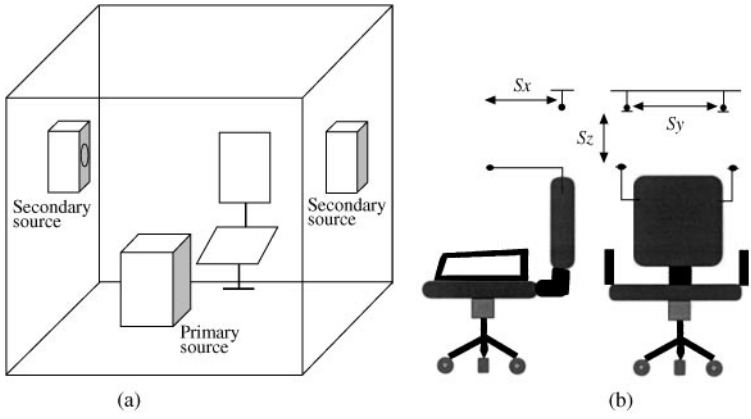

Figure 3. (a) Setting position of sources in the reverberant room; (b) seat and microphones layout (De-Diego and Gonzalez).

4. EXPERIMENTS

Experiments were carried out in the aforementioned environments. Different configurations have been chosen to demonstrate the ability of the ANC system to create *zones of quiet*. Since quiet zones are volumes in space, results are shown at different height planes (different z co-ordinates). Zones of quite are obtained by sampling an area of approximately $700 \times 500\ \text{mm}^2$ around the headrest of the seat with a monitor microphone. The objective was to obtain a large enough zone of quiet centered in the listener's head position. The effect of active control has been also evaluated in terms of the power spectral density of the signal measured at the system error sensors.

4.1. LISTENING ROOM

As a first approach, power spectral density was measured at the error sensors for different configurations. The primary signals to be cancelled were random noise and engine noise. These experiments allowed one to test the performance of the algorithms at the different control points, before analyzing the area around each error sensor. Consider a control system with 1 primary source, 1 secondary source and 2 error sensors (1 : 1 : 2 configuration). Two error sensors are located on both sides of the headrest and $S_y = 40$ cm (distance between them). The secondary source is placed at (2·4, 2·3, 1·3) m. The disturbance signal is engine noise (obtained at 1200 r.p.m., repetitive signal with harmonics of 20 Hz). The power spectral density of the signals measured at both error sensors by using the MELMS can be seen in Figure 4. There was a general attenuation around 30 dB at 100 and 120 Hz harmonics, although these reductions tend to decrease at very low frequencies because of the poor loudspeaker responses at those frequencies and around 150 Hz also due to the effect of the sampling and reconstruction filters.

In a second experiment, two secondary sources were used in order to cancel random noise (1 : 2 : 2 configuration). The power spectral density obtained at one error sensor after having used the three algorithms described in section 2 is shown in Figure 5. The ANC system achieves reduction in random noise levels at the error sensor for almost all the frequencies considered. In the same way, noise reduction levels obtained with the MELMS, LMMS and scanning error-LMS algorithms are very similar, see Figure 5(a)–(c).

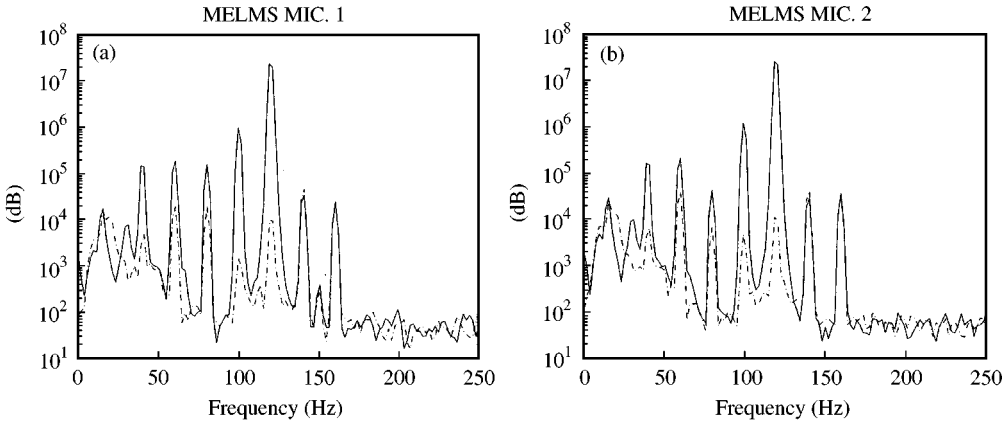

Figure 4. Power spectral density of the signal measured at the error sensors using a 1:1:2 system in the real room before the ANC system operation (solid line) and after the ANC system operation (dashed line). Engine noise and MELMS algorithm. Cut-off frequency of the filters: 150 Hz. Order of the FIR filters used on the controller was 16. (Arbitrary units) (De-Diego and Gonzalez).

The next evaluation of the multichannel system used four error sensors and two secondary sources; this configuration is called a 1:2:4 system. The loudspeakers and microphones arrangement is shown in Figure 3 ($S_z = 0$ in this case). Comparing the power spectral density obtained by using the scanning error-LMS and LMMS algorithms with the MELMS algorithm a very similar behavior is observed, not only for engine noise, see Figure 6(a)–(c) but also for random noise, see Figure 6(d)–(f).

By comparing Figure 5(a)–(c) with Figure 6(d)–(f), it can be observed how random noise levels are reduced in both configurations using the algorithms under study. However, the noise levels are slightly different. In order to justify this difference, it must be noted that the working conditions were different in both experiments. The number and arrangement of error sensors were not the same, the experiments were carried out at different dates and the noise levels that are shown were measured at different error sensors. This fact proves that the performance of active noise control systems is greatly dependent on the actual system configuration. Another important aspect that can be addressed in this experiment is which configuration can be considered the best one. Minkoff [23] proved that maximum error-reduction performance is achieved when the number of secondary sources is equal to the number of error sensors (1:2:2 configuration in the present case), provided the resulting square matrix of transfer functions between the secondary sources and the error sensors is well conditioned, which can be assumed in this case. On the other hand, rectangular (1:2:4) configurations can provide good reduction depending on other factors. The minimum mean square error for the cost function (obtained by the Wiener solution) for square systems depends only on the statistical properties of the reference and primary signals, whereas for rectangular systems, the transfer functions also come into play, not guaranteeing small residual errors. In the present experiment, both configurations provided good performance at the control points. Therefore, other properties such as availability of computational resources or the size and shape of the quite zones may allow one to choose between both configurations.

Tests were also performed using the MELMS, LMMS and scanning error-LMS algorithms in order to measure noise reduction levels in an area around the error sensors. For an increasing number of error sensors, it has been observed that quiet zones can become larger when error sensors are placed quite near (spacing used is less than $0{\cdot}1\lambda$, where

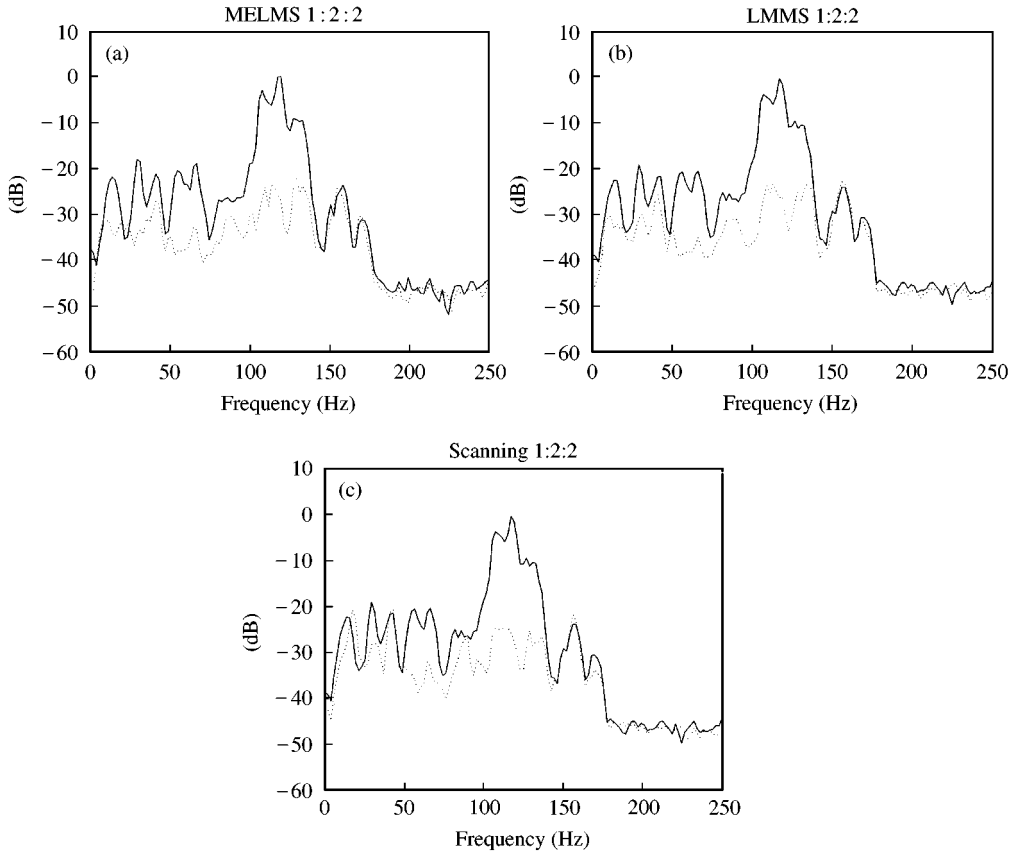

Figure 5. Power spectral density of the random noise signal measured at one error sensor using a 1:2:2 system in the real room before the ANC system operation (—— line) and after the ANC system operation (– – – – line). (a) MELMS (b) LMMS and (c) scanning error algorithms. Cut-off frequency of the filters: 150 Hz. The order of the FIR filters used on the controller was 90. (arbitrary units) (De-Diego and Gonzalez).

λ is the acoustic wavelength, for a reduction of up to 10 dB [16]) and they are moved further away from the secondary sources. Furthermore, Joseph *et al.* [4] pointed out that when error sensors are further away from the secondary source at a given frequency, the size of the zone of quiet become larger, approaching one-tenth of the wavelength of diameter limiting value. Moreover, Abbott [27] investigated how acoustical factors can limit ANC systems performance considering two simple noise field models. An interesting result of the simulations, which is related to the radial extent of the zone of quiet in a diffuse field with the secondary source located more than one-fifth of a wavelength from the primary source, showed that the high noise reduction performance is only obtained for a volume whose characteristic dimension is approximately one-tenth of a wavelength at the control point. It was also found that it is necessary to utilize multiple secondary sources in order to increase the quiet zone volume obtainable with a single secondary source. These experimental and simulated results can represent a good reference to predict to some extent the efficiency of the ANC system configuration in order to create a comfortable listening area.

Zones of quiet obtained with different error sensor arrangements for a 1:2:4 configuration are shown in Figures 7–9. Primary signals were, respectively, a single 100 Hz frequency, engine noise and random noise. Number and positions of error sensors and

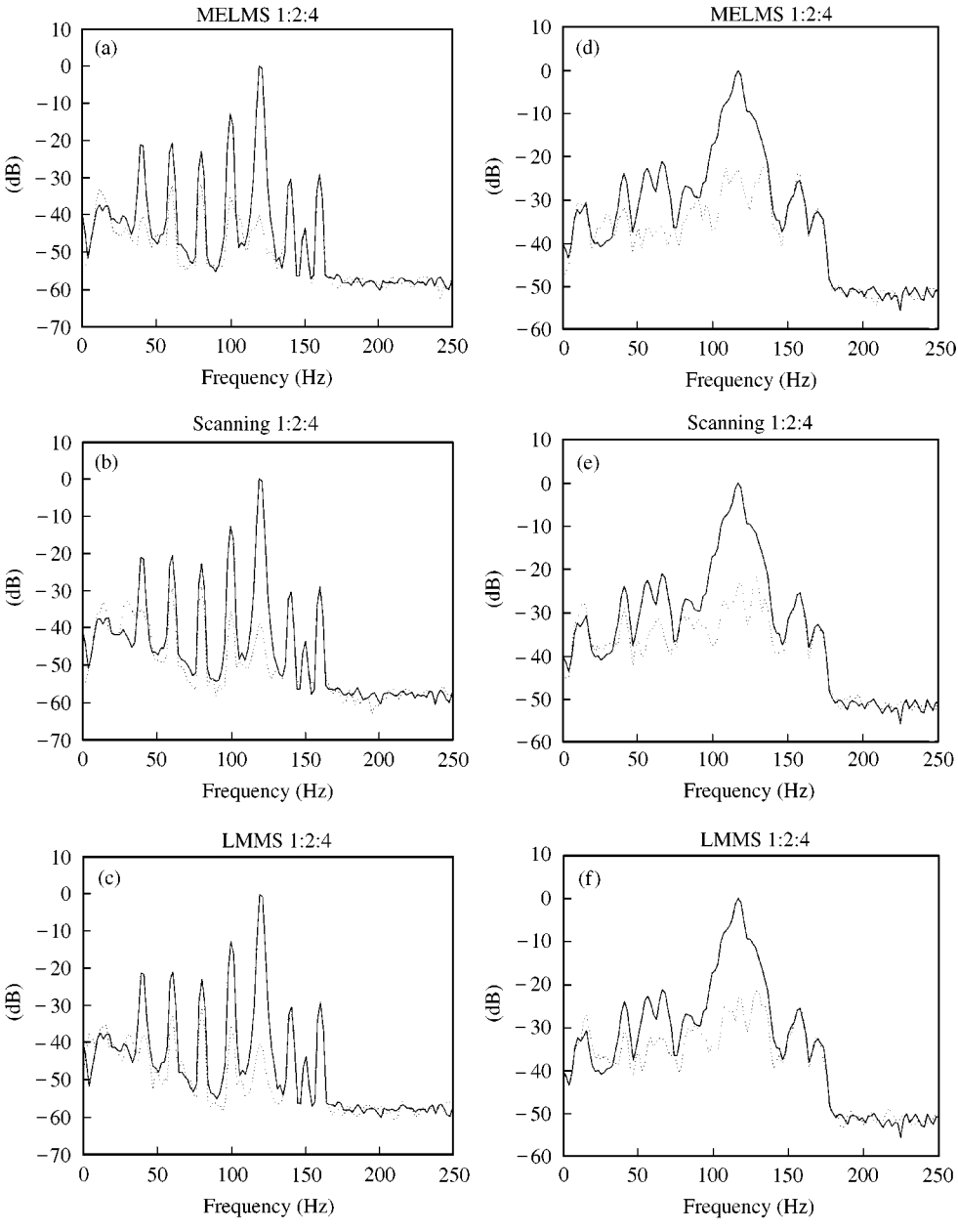

Figure 6. Power spectral density of the signal measured at one error sensor using a 1:2:4 system in the real room before the ANC system operation (—— line) and after the ANC system operation (– – – – line). Engine noise ((a)–(c)) and random noise ((d)–(f)), using, respectively, MELMS, scanning error-LMS and LMMS algorithms (arbitrary units) (De-Diego and Gonzalez).

secondary loudspeakers were chosen because it was observed that other ANC system configurations (1:1:2 and 1:2:2) provided worse results.

In Figure 7, MELMS and LMMS algorithms are used to cancel a 100 Hz pure tone in a 1:2:4 configuration. Loudspeakers were located at the same x–y plane (1·2 m in height), the secondary sources closer to the seat and on both sides of the primary source.

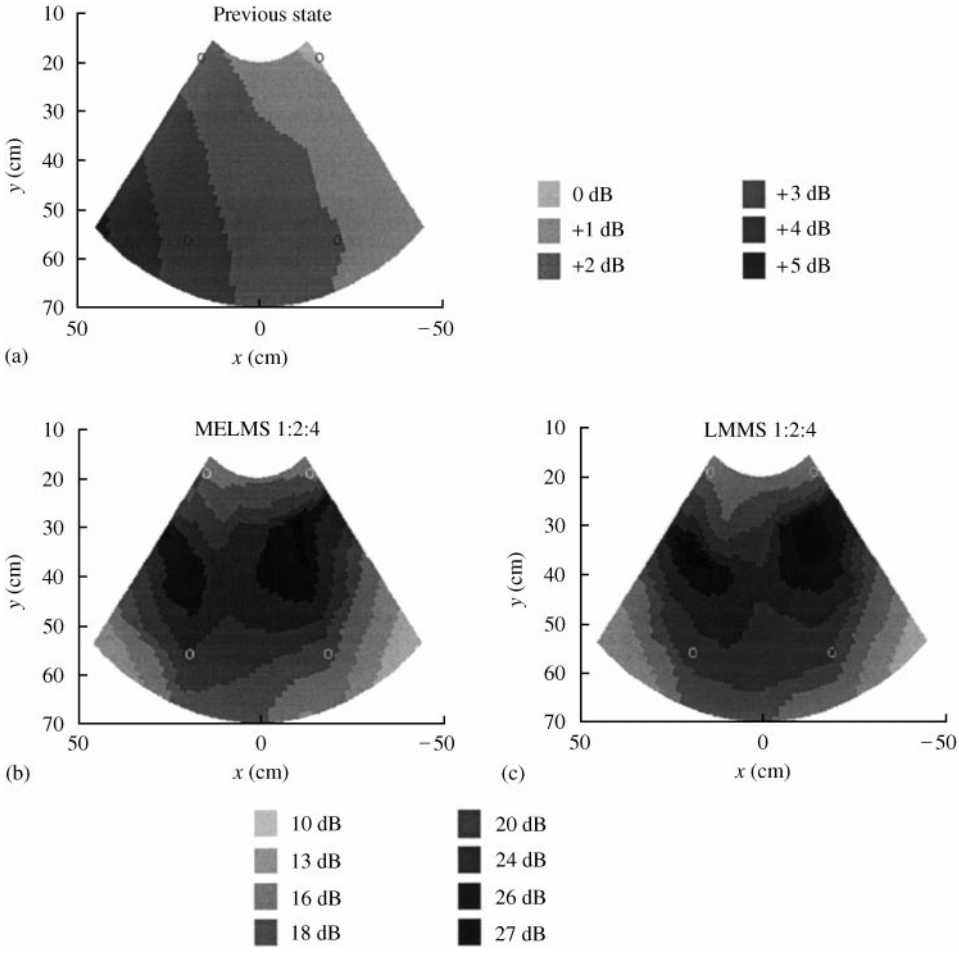

Figure 7. Attenuations achieved in a 1 : 2 : 4 system at error sensors plane after the ANC system operation using the MELMS and the LMMS algorithms in order to cancel a 100 Hz tone: (a) noise levels before cancellation, (b) MELMS algorithm results and (c) LMMS algorithm results. Circles show relative sensors position. Real room (De-Diego and Gonzalez).

Microphones were situated on the loudspeakers diaphragm plane; however, not all of them picked up the same acoustic pressure, differences were under 6 dB; see Figure 7(a). It was experimentally tested that this arrangement of transducers is optimal compared with other 1 : 2 : 4 configurations in terms of the quiet zone obtained at the plane of the listener ears. Some reasons seem to justify this fact: all the error microphones are on the same x–y plane ($z = 1{\cdot}2$ m, listener ears plane) and spacing between them is around $0{\cdot}1\lambda$ at 100 Hz; therefore they are quite close together to provide a useful-size zone of quiet. Furthermore, secondary sources (symmetrically located around the primary source) have a suitable location in order to excite those acoustic modes also excited by the primary source [3]. Finally, due to the symmetrical configuration of the system elements, the output acoustic power of the loudspeakers is quite similar, avoiding excessive power requests in the secondary sources which could produce undesirable non-linear effects. Noise reduction levels achieved by using both algorithms are shown in Figure 7. No remarkable differences were perceived in the quiet zones. Circles show error microphones positions. It can be seen in Table 2 that the

TABLE 2

Acoustic pressure levels measured at error microphones after cancellation (relative to the lowest pressure level); system, 1:2:4; listening room; cut-off frequency of 150 Hz

Microphone	MELMS (dB)	LMMS (dB)
Front right	0	1·2
Front left	1·9	0·37
Rear right	0	1·6
Rear left	1·9	1·6

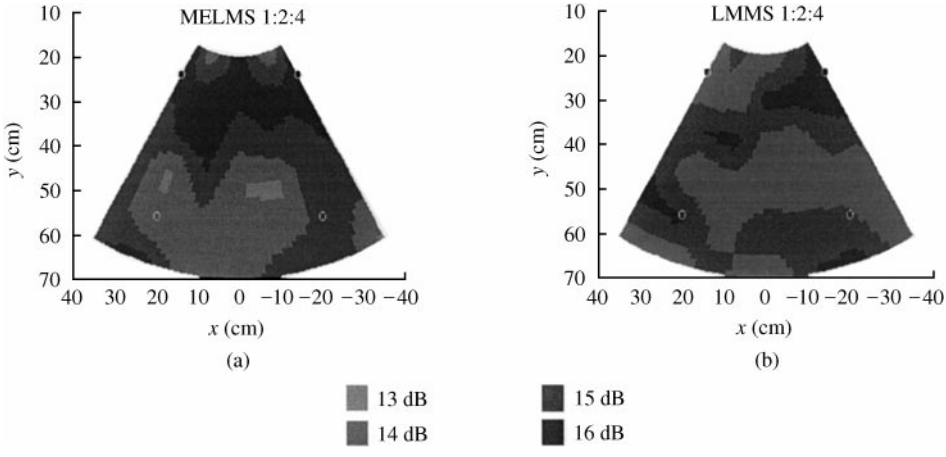

Figure 8. Attenuations achieved in a 1 : 2 : 4 system after the ANC system operation in order to cancel random noise using: (a) the MELMS algorithm or (b) the LMMS algorithm. Real room (De-Diego and Gonzalez).

MELMS algorithm strives to reduce acoustic pressure at microphones with higher levels (the right-side ones), as long as the LMMS algorithm achieves more uniform final levels. Notice that the zones of quiet attenuation are computed as the difference between the level of the acoustic field before and after the ANC system operation. In Figure 7(b) and 7(c), two high attenuation zones can be distinguished; these zones would probably join to form a larger single one by placing the error microphones closer. However, it has to be considered that error microphones should not disturb the listener's head motion. The size of the 10 dB zone of quiet obtained is larger than the acoustic field area represented in Figure 7(b) and 7(c) (approximately 84×84 cm^2, which has a diameter of a quarter of the working wavelength). Maximum noise reduction levels reach 27 dB. In fact, this final arrangement of microphones optimizes the listening area where a listener can move his head without noticing that the noise level increases.

Quiet zones were measured for the same 1 : 2 : 4 configuration with random noise signals, see Figure 8. The acoustic field before cancellation was quiet uniform. Figure 8 shows the attenuation achieved in the monitored area by using the MELMS and LMMS algorithms. Maximum attenuation levels are lower than those of the previous example (see Figure 7) because random noise produces a more complex field. Therefore, more loudspeakers and

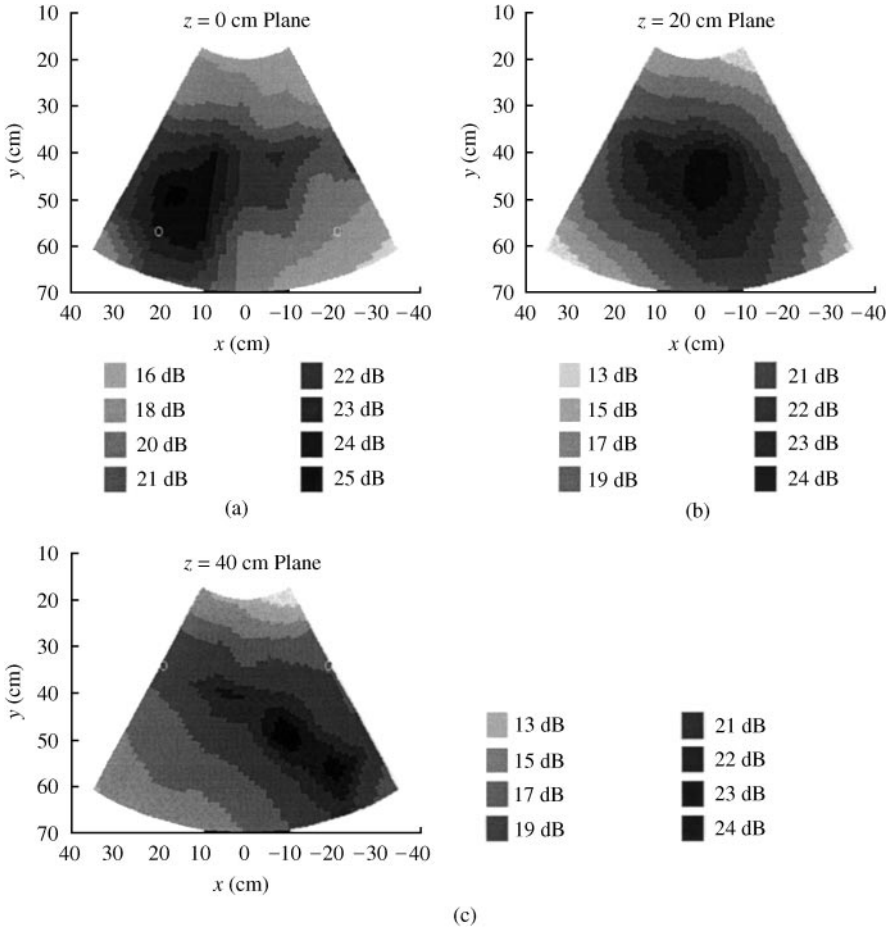

Figure 9. Attenuations achieved in a 1:2:4 system at different z planes after the ANC system operation using the MELMS algorithm in order to cancel car engine noise. (a) $z = 0$ cm plane, (b) $z = 20$ cm plane, closest to the head, (c) $z = 40$ cm plane. Real room (De-Diego and Gonzalez).

error sensors, a longer convergence time interval and a larger number of coefficients on the adaptive controller are needed in order to obtain similar performances in both experiments. Maximum noise reduction levels in the region were around 16 dB; whereas the average attenuation of the 100 Hz acoustic field was over 20 dB; see Figure 7. However, the 10 dB attenuation quiet zone is again large enough to fill the monitored area. It has to be noted that the algorithms have remained stable in spite of the presence of people moving inside the room and uncorrelated noises from other sources.

Finally, in order to test the performance of the system when the listener's head moves vertically, attenuation at different horizontal planes has been measured. Since it is desired to control actively the acoustic field of a volume in space, a different arrangement of transducers of the 1:2:4 system was shown to be required. After some laboratory trials, the final chosen placement of the loudspeakers, microphones and the seat was that shown in Figure 3 with $S_x = 30$ cm, $S_y = 40$ cm and $S_z = 40$ cm. In order to achieve more realistic results, the control system is attempting to cancel out engine noise. The MELMS algorithm is being used on the controller. All the sources were set in an horizontal plane of 1·2 m height ($z = 20$ cm) which corresponds to the listener's head position. The z-co-ordinate

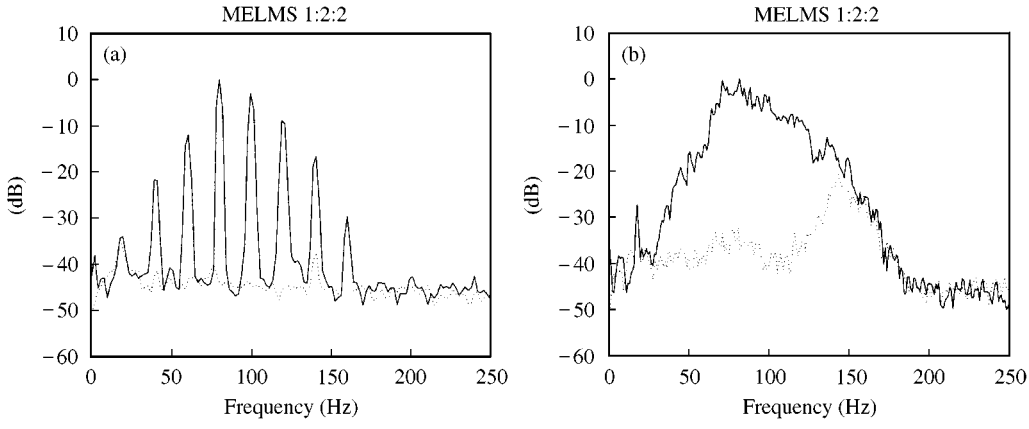

Figure 10. Power spectral density of the signal measured at one error sensor using a 1:2:2 system in semi-anechoic chamber before the ANC system operation (—— line), after the ANC system operation (– – – – line) using the MELMS. (a) Engine noise and (b) random noise. Cut-off frequency of the filters: 150 Hz (arbitrary units) (De-Diego and Gonzalez).

origin is now taken at 1·2 m height. Thus, the front error sensors are located at $z = 0$ cm and the rear ones at $z = 40$ cm. Figure 9 shows attenuation measured at three different horizontal planes. Results demonstrate that very meaningful reductions are obtained at the measurement plane closest to the plane where the listener ears were located; see Figure 9(b). The more quiet area (the darkest one) in this figure is centered, as could be desired. The other two measured planes present darkest areas that are not centered. This fact is due to the asymmetries of the system. If the listener moves his head inside the controlled volume a slight change of the perceived noise level can be appreciated. In any case the extent of the volume of quiet is large enough to allow these movements. Level reductions up to 24 dB with a mean value of around 20 dB are achieved at the three planes.

4.2. SEMI-ANECHOIC CHAMBER

A complete set of measurements was also carried out in a semi-anechoic chamber in order to know how the acoustic characteristics of an enclosure determine the performance of the ANC system. The performance comparison of the practical system in the listening room and in the semi-anechoic chamber makes it possible to somewhat predict the effect of an ANC system in an arbitrary room. Noise reduction significantly improves in the semi-anechoic chamber due to the acoustic field simplicity. Figure 10 shows the cancellation of engine and random noise when using a 1:2:2 system. Results were obtained at one error sensor by means of the MELMS algorithm. Attenuation higher than 30 dB was achieved at some frequencies. The power spectral density of random noise before and after control in both environments for a 1:2:2 system by using the MELMS can be observed in Figures 5(a) and 10(b).

Figure 11 shows the residual field that results after cancelling engine noise with a 1:2:4 system by using the MELMS and the LMMS algorithms on the controller. Despite increasing the working frequency range (cut-off frequency of 230 Hz), attenuation over 20 dB (higher reductions than in the listening room) has been achieved. Although zones of quiet obtained by using both algorithms do not show the same shape, acoustic noise levels

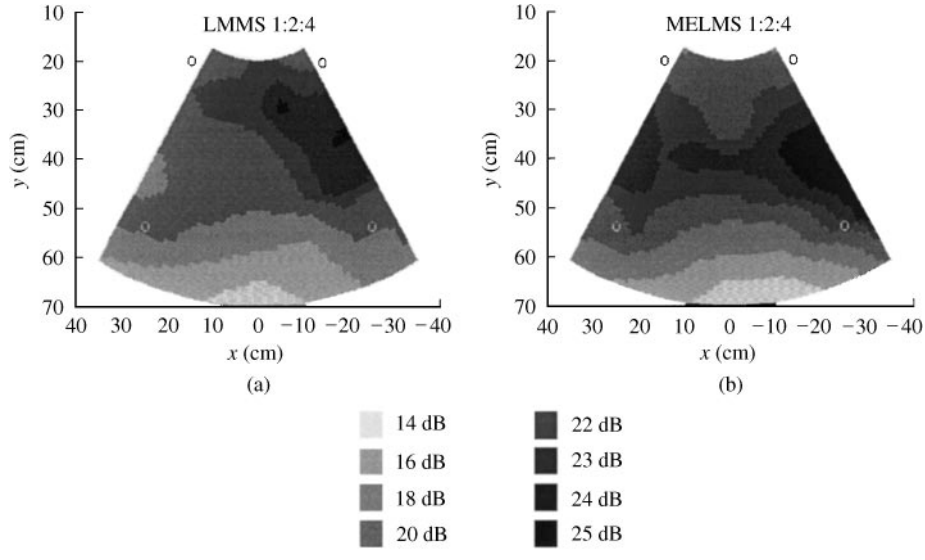

Figure 11. Attenuations achieved using a 1:2:4 system at error sensors plane after the ANC system operation in order to cancel car engine noise using: (a) LMMS algorithm and (b) MELMS algorithm. Semi-anechoic chamber. Cut-off frequency of the filters: 240 Hz (De-Diego and Gonzalez).

after cancellation are very similar. A more uniform residual acoustic field is achieved again by using the LMMS algorithm.

5. CONCLUSIONS

A multichannel system applied to a laboratory prototype for local active noise control was described. The known MELMS (multichannel version of the filtered-X LMS), LMMS and scanning error-LMS algorithms have been developed and tested on the controller. Experimental verification tests show a similar performance of the algorithms in some aspects; in particular, all of them are robust and present similar convergence rates. LMMS and scanning error-LMS algorithms reduce the computational load compared to the MELMS algorithm, since they use only one error signal at each algorithm iteration, whereas MELMS uses all the error signals. However, it has to be noted that the LMMS algorithm has to compute all the error signal powers in order to look for the maximum. This fact determines that its computational cost saving depends on the number of error sensors. If this number increases, the computational complexity of the LMMS will be similar to the MELMS complexity. On the other hand, as can be concluded from the results, the LMMS algorithm also provides a more uniform residual field compared with the MELMS and the scanning error-LMS. This behavior could have been expected since its optimization strategy is based on the minimization of the maximum error signal level.

Experiments with different configurations and different numbers of loudspeakers and error sensors were conducted. The position of the loudspeakers and sensors has been shown to be very important to achieve finally a certain acoustic field in the controlled area. Results demonstrate the possibility to adjust the size and quality of the quiet zones by optimizing the number and position of secondary sources and error sensors. From the experiments the optimum configuration of the local system for a single listener would be a 1:2:4

configuration with the error sensors located at different z planes in order to achieve larger volume of quiet and therefore allow three-dimensional movements of the listener's head. The 10 dB zones of quiet at each z plane are shown to be larger than those represented in the figures, which means at least an area of $80 \times 45\ \text{cm}^2$. The 10 dB zone of quiet generally becomes larger if the error sensors are closer, but the error sensors must not disturb head movements. Head motion and the zone of quiet extension can be improved together by minimizing the pressure at point nearer to the listener head, rather than at an error microphone placed further away. This method, which was reported in reference [5], is left as a topic of future research.

Finally, the system has been shown to be able to achieve noise reductions around the headrest of a seat placed inside an enclosure. Different kinds of noise, single frequencies, random noise and engine noise, have been attenuated. Meaningful convergence rates and stability were achieved on the ANC system in all the experiments.

REFERENCES

1. S. J. ELLIOTT and P. A. NELSON 1993 *IEEE Signal Processing Magazine* **10**, 12–35. Active noise control.
2. P. A. NELSON and S. J. ELLIOTT 1992 *Active Control of Sound*. New York: Academic Press.
3. H. KUTTRUF 1991 *Room Acoustics*. New York: Elsevier Science Publishers Ltd.; third edition.
4. P. JOSEPH, S. J. ELLIOTT and P. NELSON 1994 *Journal of Sound and Vibration* **172**, 605–627. Near field zones of quiet.
5. J. GARCIA-BONITO, S. J. ELLIOTT and C. C. BOUCHER 1997. *Journal of the Acoustical Society of America* **101**, 3498–3516. Generation of zones of quiet using a virtual microphone arrangement.
6. S. KUO and D. MORGAN 1996 *Active Noise Control Systems*. New York: John Wiley & Sons.
7. S. J. ELLIOTT, I. M. STOTHERS and P. A. NELSON 1987 *IEEE Transactions on Acoustical Speech and Signal Processing* **35**, 1423–1434. A multiple error LMS algorithm and its application to the active control of sound and vibration.
8. A. GONZALEZ, S. J. ELLIOTT and A. ALBIOL 1997 *Proceeding of the International Conference on Acoustics, Speech and Signal Processing* (*ICASSP*) **1**, 1–4. Minimisation of the maximum error signal in active control.
9. H. HAMADA 1991 *Proceedings of the International Symposium on Active Control of Sound and Vibration* **1**, 33–44. Signal processing for active noise control: adaptive signal processing.
10. A. GONZALEZ 1998 *Proceedings of the European Signal Processing Conference* (*EUSIPCO*) IV, 2333–2336. Stochastic gradient algorithms in active control.
11. A. GONZALEZ, A. ALBIOL and S. J. ELLIOTT 1998 *IEEE Transactions on Speech and Audio Processing* **6**, 268–281. Minimisation of the maximum error signal in active control.
12. M. TANAKA, S. MAKINO and J. KOJIMA 1999 *IEEE Transactions on Speech and Audio Processing* **7**, 79–86. A block exact fast affine projection algorithm.
13. H. SANO, S. ADACHI and H. KASUYA 1997 *Journal of Dynamic Systems, Measurements and Control. Transaction of the American Society of Mechanical Engineers* **119**, 318–320. Application of a least squares lattice algorithm to active noise control for an automobile.
14. O. S. KWON and I. W. CHA 1998 *Electronic Letters* **34**, 1559–1560. Multichannel optional summed algorithm for active noise control.
15. H. JANOCHA and B. LIU 1998 *IEE Proceedings—Control Theory Application* **145**, 423–426. Simulation approach and causality evaluation for an active noise control system.
16. W. DRUYVESTEYN and J. GARAS 1997 *Journal of the Audio Engineering Society* **45**, 685–701. Personal sound.
17. S. HAYKIN 1996 *Adaptive Filter Theory*. Upper Saddle River, NJ: Prentice-Hall.
18. B. WIDROW and S. D. STEARNS 1985 *Adaptive Signal Processing*. Englewood Cliffs, NJ: Prentice-Hall.
19. A. GONZALEZ 1997 *Applied Signal Processing*, Vol. 4, 94-106. London: Springer-Verlag. Multiple error algorithms for feedforward active noise control in ducts.
20. S. J. ELLIOTT, C. BOUCHER and P. A. NELSON 1992 *IEEE Transactions on Signal Processing* **40**, 1041–1052. The behaviour of a multiple channel active control system.

21. S. J. ELLIOTT *et al.* 1998 *Proceedings of Inter-Noise* '88, 987–990. The active control of engine noise inside cars.
22. S. J. ELLIOTT, I. M. STOTHERS and C. C. BOUCHER 1990 *Journal of Sound and Vibration* **140**, 219–238. In flight experiments on the active control of propeller-induced cabin noise.
23. J. MINKOFF 1997 *IEEE Transactions on Signal Processing* **45**, 2993–3005. The operation of multichannel feedforward adaptive systems.
24. S. C. DOUGLAS 1997 *Proceedings of the International Conference on Acoustical Speech and Signal Processing* (*ICASSP*), Vol. 1, 399–402. Fast exact filtered-X LMS and LMS algorithms for multichannel active noise control.
25. S. C. DOUGLAS 1997 *Proceedings of the National Conference Noise Control Engineering*, Vol. 2, 209–220. Reducing the computational and memory requirements of the multichannel filtered-X LMS adaptive controller.
26. A. GONZALEZ 1997 *Ph.D. Thesis, Technical University of Valencia.* Active control of noise using adaptive signal processing (in Spanish).
27. J. F. ABBOTT 1993 *Transactions of IEEE* 0-7803-0946-4/93, V-630-633. Acoustical design criteria for active noise control systems.